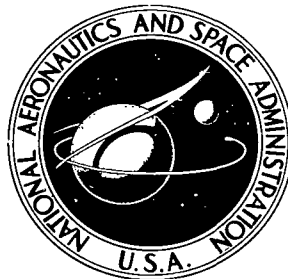


**NASA TECHNICAL NOTE**



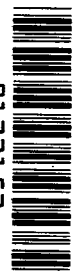
**NASA TN D-6626**

*0.1*

**NASA TN D-6626**

**LOAN COPY: RETURN  
AFWL (DOUL)  
KIRTLAND AFB, N.**

0133153



**TECH LIBRARY KAFB, NM**

# **DIMENSIONAL-STABILITY STUDIES OF CANDIDATE SPACE-TELESCOPE MIRROR-SUBSTRATE MATERIALS**

*by John M. Jerke and Robert J. Platt, Jr.*

*Langley Research Center*

*Hampton, Va. 23365*

**NATIONAL AERONAUTICS AND SPACE ADMINISTRATION • WASHINGTON, D. C. • JANUARY 1972**



0133153

1. Report No. NASA TN D-6626	2. Government Accession No.	3. Recipient's Catalog No.	
4. Title and Subtitle DIMENSIONAL-STABILITY STUDIES OF CANDIDATE SPACE-TELESCOPE MIRROR-SUBSTRATE MATERIALS		5. Report Date January 1972	
		6. Performing Organization Code	
7. Author(s) John M. Jerke and Robert J. Platt, Jr.		8. Performing Organization Report No. L-7727	
		10. Work Unit No. 188-78-57-01	
9. Performing Organization Name and Address NASA Langley Research Center Hampton, Va. 23365		11. Contract or Grant No.	
		13. Type of Report and Period Covered Technical Note	
12. Sponsoring Agency Name and Address National Aeronautics and Space Administration Washington, D.C. 20546		14. Sponsoring Agency Code	
		15. Supplementary Notes	
16. Abstract  The effects of aging, vacuum exposure, and thermal cycling on the dimensional stability of mirror-substrate materials – fused silica, Cer-Vit, Kanigen-coated beryllium, polycrystalline silicon, and U.L.E. fused silica – were investigated. A multiple-beam interferometer was used to determine nonrecoverable surface-shape changes of the 12.7-cm-diameter mirrors with substrates of these materials. Thermal cycling and aging in vacuum produced the largest changes, but only a few were as large as 1/30 wavelength, where the wavelength was 632.8 nm.			
17. Key Words (Suggested by Author(s)) Mirror-substrate materials Space telescope		18. Distribution Statement Unclassified – Unlimited	
19. Security Classif. (of this report) Unclassified	20. Security Classif. (of this page) Unclassified	21. No. of Pages 23	22. Price* \$3.00

# DIMENSIONAL-STABILITY STUDIES OF CANDIDATE SPACE-TELESCOPE MIRROR-SUBSTRATE MATERIALS

By John M. Jerke and Robert J. Platt, Jr.  
Langley Research Center

## SUMMARY

The effects of aging, vacuum exposure, and thermal cycling on the dimensional stability of five candidate mirror-substrate materials for a proposed large-diameter space telescope were investigated. The substrate materials include fused silica, Kanigen-coated beryllium, Cer-Vit, polycrystalline silicon, and U.L.E. fused silica. The test samples were 12.7-cm-diameter optical flats of the substrate material coated with aluminum and either magnesium fluoride or silicon oxide. A multiple-beam interferometer was used to determine nonrecoverable surface-shape changes to about  $1/40$  wavelength, where the wavelength was 632.8 nm, for the test mirrors. One set of mirrors was kept at room conditions for about 7 months; a second set was placed in a vacuum for 6 months; and a third set was subjected to thermal cycles from room temperature to a maximum of 418 K and from room temperature to a minimum of 195 K.

Stabilities of the mirrors aged at room conditions appeared similar, with surface changes, if any, less than  $1/40$  wavelength. Vacuum aging and thermal cycling produced larger nonrecoverable changes, but none exceeded  $1/30$  wavelength.

## INTRODUCTION

Earth-orbiting telescopes offer considerable advantages over those used in ground-based observatories. The absence of an atmosphere at orbital altitudes results in observational freedom from both optical turbulence and spectral absorption. Without the degrading effect of optical turbulence, the image quality of the space telescope is determined primarily by the figure (surface shape) of the optical elements and the pointing stability of the telescope. (See ref. 1.)

In proposed configurations for a large-diameter space telescope, mirrors, for the most part, have been considered the principal optical elements. To attain the required high resolution from the telescope, the figure of the primary mirror can be permitted to depart from the design shape by no more than  $\lambda/50$  rms (ref. 1), where  $\lambda$  is the wavelength of the radiation. Expressed as a peak-to-valley deviation, the permissible error

is several times as large, or about  $\lambda/15$ . Therefore, a prime consideration in the selection of a mirror-substrate material is its ability to retain its figure during the telescope lifetime. A uniform change in the mirror dimensions changes the mirror focal length but should not be a serious problem, as a correction may be made. The serious problem is nonuniform changes, which may be due to the long-term release of stored energy (such as the gradual relaxation of residual stresses during the telescope lifetime), to temperature changes, and perhaps to other effects of the space environment.

Reference 2 reported the results of an investigation into the temporal (aging) and thermal stability of several candidate mirror-substrate materials. Interferometric measurements of mirror-figure changes were presented, including the nonrecoverable change produced by repeated temperature cycling through a range of 11 K.

The purpose of the present investigation was to examine the effects of a vacuum exposure and the effects of larger amplitude thermal cycling on the dimensional stability of several of these same candidate mirror-substrate materials. The materials tested were fused silica, beryllium with an electroless nickel coating (beryllium-Kanigen), Cer-Vit, polycrystalline silicon, and U.L.E. fused silica. Mirror-figure changes resulting from aging in both atmospheric and vacuum environments, and the nonrecoverable changes resulting from thermal cycling were examined. Thermal cycling extended both above and below room temperature through a maximum range of about 220 K.

A multiple-beam interferometer was used to make interferograms of the mirror surfaces. Mirror-figure changes were determined by a visual comparison of interferograms. A more detailed examination of selected pairs of interferograms was made under contract using an automated analysis technique.

## TEST MIRRORS

Table I gives the substrate materials, substrate manufacturers, and coatings for the 17 test mirrors. The substrate materials were fused silica, beryllium-Kanigen, Cer-Vit, polycrystalline silicon, and U.L.E. fused silica. Cer-Vit and U.L.E. fused silica are a glass ceramic and titanium-silicate glass, respectively, with near-zero coefficients of thermal expansion at room temperature. The beryllium substrates were made of instrument-grade material produced by the hot-pressing of beryllium powder. Kanigen coating (electroless nickel), 0.1 mm thick, was applied to both sides of each beryllium substrate to provide a material better suited for polishing. The test mirrors were 12.7 cm in diameter and 1.9 cm thick, with one surface polished and vacuum coated with a 70- to 150-nm thickness of aluminum (Al). The aluminized surfaces were overcoated with a 25-nm thickness of magnesium fluoride ( $\text{MgF}_2$ ) at a substrate temperature of about 550 K, except for three fused-silica substrates which were overcoated with a 250-nm thickness of silicon oxide ( $\text{Si}_2\text{O}_3$ ), as described in reference 3.

## EXPERIMENTAL PROCEDURE

### Interferometry

A multiple-beam interferometer (ref. 4) was used to determine changes in flatness of the test mirrors. A photograph and a schematic of the interferometer with a test mirror in place are shown in figures 1 and 2, respectively. This type interferometer produces an interference pattern from multiply reflected light in an air wedge between the reflective surfaces of the test mirror and a coated reference flat. The metallic coating on the reference flat is thin enough to be partially transparent. The advantage of this type of interferometer over the type with two beams is that narrower, sharper fringes are produced, which greatly improve the sensitivity of the measurement. The reference flat, made of Corning fused silica No. 7940, was 15.2 cm in diameter and approximately 1.9 cm thick. It was made with a built-in wedge angle to eliminate fringes formed by the interference of reflections from its two surfaces. The reference surface was vacuum coated with aluminum to allow 10 percent of an incident beam to be transmitted.

The test mirror was mounted vertically in a circular metal mount. The mirror was supported within the mount by three rubber pads. The upper pad was adjustable to hold the mirror in the mount. The test mirror could be rotated about vertical and horizontal axes by means of differential screws on the mount to control the number and orientation of the fringes.

Monochromatic light, with a wavelength of 632.8 nm, from a 5-mW He-Ne (helium-neon) laser equipped with an expanding lens, was collimated by a paraboloidal mirror with a 3-meter focal length. This beam was directed at the test mirror and reference flat at near-normal incidence. The reflected beam, which contained the interference fringe pattern, was reduced in size by a second paraboloidal mirror and the fringe pattern recorded on photographic film and also displayed on a viewing screen.

Interferograms of the test mirrors were made at the intervals during the aging and before and after the vacuum exposure and each thermal-cycling test. To make an interferogram, the test mirror in the mount was positioned with the reflective surface close to that of the reference flat, and the wedge angle between the two was decreased until fringes appeared on the viewing screen. When comparison with an earlier interferogram was desired, an image of the earlier interferogram was superimposed on the fringe pattern by means of a projector. The mirror was then adjusted to bring the fringes into coincidence with the projected pattern as closely as possible, and the film shutter was released. The ambient temperature during the taking of interferograms was between 296 and 303 K.

Typical mirror interferograms are shown in figure 3. Interferograms with fringes running vertically and horizontally across the mirror surface, as shown in figures 3(a)

and 3(b), respectively, were generally taken for each mirror and hereafter will be referred to as vertical and horizontal interferograms. The two tick marks at the top and bottom of each interferogram are fiducial marks used for alining interferograms for comparison. If the reflective surfaces of the test mirror and reference flat were perfectly flat, the fringes would be straight and equally spaced for any orientation of the interference pattern. Curvature and unequal spacing of the fringes are introduced by deviations from plane surfaces of the test mirror and reference flat. Since mirror-figure changes, not absolute mirror figures, were to be determined, the reference surface was not required to be optically flat.

Interferograms made before and after an environmental test were compared to determine if any change in the mirror figure had taken place. A visual inspection was made by superimposing the interferograms, which were positive prints, over a light box in a darkened room. The fringes were slightly displaced in order that one set did not mask the other set. Such a superposition was made with transparencies made from the original prints and is shown in figure 4. Figure 4(a) shows the superposition of interferograms of a beryllium-Kanigen mirror taken before and after 160 thermal cycles. The similarity of the two sets of fringes indicates that no significant change took place. Figure 4(b) shows the superposition of interferograms of a U.L.E. fused-silica mirror subjected to the same thermal cycles. Changes in both curvature and spacing between the two sets of fringes are evident for both horizontal and vertical fringe orientation. The maximum difference in the shape and spacing of one set of fringes relative to the other may be expressed in terms of the wavelength of light (one fringe space represents a displacement normal to the plane of the mirror of  $\lambda/2$ ). Visual comparison of the interferograms used for figure 4(b) indicated that the mirror figure changed as much as  $\lambda/30$ .

More detailed measurements of a few selected interferogram pairs were made under contract by an automated analysis technique. This analysis used numerical methods similar to those reported in reference 5 and produced a contour map of the mirror-figure change corresponding to the interferogram changes, the maximum peak-to-valley change, and the root-mean-square value of the interferogram changes. The automated analysis technique is described in the appendix.

It should be realized that an observed change in fringe shape and spacing (possibly approaching  $\lambda/40$ ) may have been produced by other than a change in the figure of the test mirrors. External factors which could have affected the fringes are reference-flat and test-mirror vibrations, temperature variations, differences in mirror mounting forces, and changes in the reference flat. For the data presented, mounting forces and vibration were minimal, and time was allowed for temperature to stabilize after mounting the mirror. Nonetheless, some effects of these factors may still have existed. For this reason,

changes of less than  $\lambda/40$ , although observable in the interferograms, are thought to be within the error of measurement.

### Environmental Tests

The environmental testing of the mirrors consisted of aging at room conditions, vacuum exposure, and thermal cycling. The mirror samples were separated into three sets with one mirror of each type (substrate plus coatings) in a set (except for the atmospheric aging tests which did not include a silicon mirror), and all the mirrors of a set were exposed or cycled simultaneously.

Aging in atmosphere.- A set of five mirrors was kept in a laboratory cabinet during the test program. In addition to using this set of mirrors to monitor the effects of aging on the mirror figures, these mirrors served as standards for the other two sets of test mirrors. The ambient temperature of the standard mirrors was maintained between 293 and 303 K during the test program. Interferograms were recorded periodically over a period of about 7 months.

The first set of interferograms taken with the multiple-beam interferometer was made 21 months after receipt of the test mirrors from the supplier. Therefore, possible aging effects on the mirror figures during the period immediately after mirror preparation were not determined. However, dimensional stability tests reported in reference 2 did show that a fused-silica mirror became progressively more stable over a 30-month period following mirror preparation.

Aging in vacuum.- One set of six mirrors was placed in an ion-pumped vacuum chamber for two periods of approximately 6 months each. Interferograms made with the multiple-beam interferometer were obtained only for the second vacuum exposure. A period of approximately 8 months elapsed between receipt of the mirrors and the first vacuum exposure, and a period of 5 months elapsed between the two vacuum exposures. Several days elapsed between removal of the mirrors from the vacuum chamber and making the interferograms.

The test mirrors were set on stainless-steel plates in the vacuum chamber, and the chamber pressure was maintained at approximately  $10^{-8}$  N/m<sup>2</sup> throughout the test period. Thermocouples welded to the steel plates indicated a temperature of  $297 \pm 3$  K for both vacuum exposure periods.

Thermal cycling.- In the thermal-cycling tests, the mirrors were subjected to alternate sets of heating and cooling cycles, as shown in table II. No attempt was made to simulate the thermal cycle a particular space telescope might undergo. Instead, the mirrors were subjected to increasingly large thermal cycles to determine if any of these materials were significantly better than the others in dimensional stability. Each test

consisted of 10 cycles, except for one test of 80 heat cycles from 303 to 321 K. The temperature ranges given in table II are average values. Individual cycles may have varied as much as 4 K from these values.

Heat-cycle tests were conducted by placing the test mirrors in a forced-air-circulation oven with subsequent heating and cooling. Each mirror was wrapped in several layers of paper to ensure gradual heating and cooling. For most of the heat-cycle tests, thermocouples were attached to the nonreflective sides of selected mirrors, and the mirror temperatures were recorded. Typical mirror temperatures during the heating and cooling phases of cycling from 306 to 418 K are presented in figure 5 for the fused-silica and beryllium-Kanigen mirrors. After each set of heating cycles, the mirrors were removed from the oven and allowed to reach room temperature before interferograms were taken.

Cooling-cycle tests were conducted by placing the mirrors in a refrigerator for cycling from room temperature to 271 K and in a bath with dry ice added for all other cooling cycles. Each mirror was wrapped in paper and sealed in several plastic bags. The most rapid temperature change experienced by the mirrors occurred when the bags containing the mirrors were immersed in a 243 K bath of ethylene glycol. The surface temperature measured for a fused-silica mirror during this cooling cycle is shown in figure 6(a). For lower temperature cycles, the mirrors were placed in a room-temperature bath of acetone and dry ice was then added. The mirror-surface temperature measured for the coldest cycle is shown in figure 6(b).

## RESULTS AND DISCUSSION

The maximum fringe changes observed by comparison of interferogram pairs taken of the mirrors before and after aging in the atmosphere and in a vacuum and after thermal cycling are presented in table III. These changes, expressed as apparent mirror-figure changes, were determined from a visual comparison of interferograms. Changes are shown in many cases for both vertical and horizontal interferograms. Table III(a) gives maximum fringe changes for intermediate aging periods obtained by comparison of interferograms taken just before and after a given period. The last column gives the overall changes, obtained by comparison of the original interferograms with ones taken at the end of the 222-day aging test. Table III(b) gives the observed changes after an exposure of another set of mirrors to high-vacuum conditions for 186 days. Table III(c) gives changes produced by the different sets of thermal cycles on a third set of test mirrors at intermediate periods. Usable data were not obtained for the first set of 10 thermal cycles. The last column gives the overall changes obtained by comparison of the interferograms made before the start of the second set of thermal cycles with those made after completion of all 170 cycles. Most of the interferogram changes shown in table III

were obtained by visual comparison of pictures. However, the maximum peak-to-valley changes, as determined by an automated analysis method (see appendix), are also given in the table. These peak-to-valley changes are in good agreement with the fringe changes obtained by the visual comparison.

As shown in table III(a), interferogram fringe changes of as much as  $\lambda/40$  were found in a few instances. Other measurements, which indicated changes less than  $\lambda/40$ , or for which no change could be detected, are listed in the table as  $<\lambda/40$ . For most mirrors, a change as large as  $\lambda/40$  was indicated only by the vertical interferograms and was not corroborated by the horizontal interferograms. For the overall aging period (last column), no change this large was noted in either vertical or horizontal interferograms. Therefore, the few  $\lambda/40$  fringe changes noted for intermediate aging periods may not represent true mirror changes but may instead be the result of vibration or other external influences which could affect the position of the fringes. In summary, the temporal stabilities of these substrates appear to be similar; changes in mirror figure, if any, were less than  $\lambda/40$  for the 7-month period. (It should be noted that a silicon mirror was not available for the atmospheric aging test.)

The results of the second vacuum exposure period of 186 days, presented in table III(b), show more fringe changes than were found for the atmospheric aging test. Fringe changes of  $\lambda/40$  for one of the fused-silica mirrors and the beryllium-Kanigen mirror were apparent in the vertical interferograms but were not corroborated by the horizontal interferograms. Fringe changes of at least  $\lambda/40$  were found for the Cer-Vit and silicon mirrors for both orientations of the fringes, and these latter mirrors evidently did experience a true figure change for the 6-month vacuum test.

The results of the thermal-cycling tests, presented in table III(c) show numerous fringe shifts of  $\lambda/40$  by the visual comparison method and a few of as much as  $\lambda/30$ . For most mirrors, these changes were apparent in both horizontal and vertical interferograms and are thought to approximate the true mirror-figure changes. The Cer-Vit and U.L.E. fused-silica mirrors showed the most numerous changes of  $\lambda/40$  or more during the cycling and the silicon mirror showed no such changes. The changes indicated after a set of heat cycles were often reversed by the next set of cooling cycles. The overall change, at the end of the cycling, was then not large for any of the mirrors. The maximum overall change was about  $\lambda/30$  by both the visual comparison method and the automated analysis.

The results given in table III for aging, vacuum exposure, and thermal cycling indicate that the mirrors made of hot-pressed beryllium with a Kanigen coating on both sides were as stable as any substrate materials tested. This result was unexpected in view of previous tests (ref. 6) which indicated that hot-pressed beryllium with a nickel coating on only one surface was temporally unstable. Other tests (ref. 7) have

shown that the electroless nickel coating on beryllium induces stresses which adversely affect the material stability. Having the Kanigen coating on both surfaces of the beryllium, as in the present tests, apparently reduced this instability. Another factor tending to reduce the observed instability was the 21-month time lapse between mirror fabrication and testing.

The dielectric mirrors (Cer-Vit, U.L.E. fused silica, and fused silica) have about the same stability with an indicated figure change no greater than  $\lambda/30$ , based on the visual comparison method. The silicon mirror subjected to thermal cycling was very stable; however, the silicon mirror exposed to the vacuum did indicate a change of at least  $\lambda/40$ . In general, the mirrors had dimensional stabilities approaching the limit of detection of the interferometer, with only a few changes exceeding  $\lambda/40$ .

### CONCLUSIONS

The dimensional stability of 12.7-cm-diameter flat mirrors with substrate materials of fused silica, Kanigen-coated beryllium, Cer-Vit, polycrystalline silicon, and U.L.E. fused silica was investigated by aging, vacuum exposure, and thermal cycling. Mirror interferograms taken before and after each environmental exposure were compared to estimate nonrecoverable figure changes to  $1/40$  wavelength, where the wavelength was 632.8 nm. This comparison indicated the following:

1. The dimensional stabilities of the mirrors examined for the effects of aging at room conditions appeared to be similar. Changes in mirror figure, if any, were less than  $1/40$  wavelength for the 7-month period.
2. Mirror-figure measurements made before and after a vacuum exposure of 6 months indicated a greater effect on the Cer-Vit and silicon mirrors, which changed about  $1/40$  wavelength, than on the other substrates of this set of mirrors.
3. Thermal cycling over a range of 195 to 418 K of a third set of mirrors produced little or no figure change for the silicon substrate. Changes in the other mirrors were scattered throughout the course of the thermal cycling, with no change exceeding  $1/30$  wavelength, as determined by the visual method.
4. The expected instability of the Kanigen-coated beryllium mirrors was not detected. Their good behavior may have been due to the Kanigen coating being applied to both front and back surfaces and to the 21-month time between mirror fabrication and testing.

5. In general, the mirrors had dimensional stabilities approaching the limit of detection of the interferometer, with only a few changes exceeding  $1/40$  wavelength.

Langley Research Center,  
National Aeronautics and Space Administration,  
Hampton, Va., December 20, 1971.

## APPENDIX

### QUANTITATIVE ANALYSIS OF INTERFEROGRAMS

In addition to a visual analysis of test-mirror interferograms, a quantitative analysis using numerical methods similar to those reported in reference 5 was performed under contract on selected interferograms. This automated interferogram-analysis technique furnished the following information: (1) peak-to-valley and root-mean-square data on the mirror-surface figure, (2) contour map of the mirror surface, (3) root-mean-square and maximum peak-to-valley values for the differences between two interferograms taken before and after an environmental test, and (4) a contour map of the mirror-figure changes.

Transparencies were made of the original interferograms and furnished the contractor, who scanned them with a microdensitometer to locate the fringe positions. The automated technique for analyzing an interferogram consisted primarily of a high-speed electronic-computer program to perform the following steps: (1) assign a constant optical-path difference to all scan points lying on the same fringe; (2) calculate a series of parallel, equally spaced, straight lines that best fit all the optical-path differences for the mirror in a root-mean-square sense; (3) determine for each fringe the differences, or residual optical-path differences, between the assigned optical-path difference and the best fitting straight line; (4) calculate the optical-path difference at each point of a grid over the mirror aperture by interpolating from the surrounding data points; and (5) produce a contour map of the mirror surface. For a pair of interferograms representing a mirror figure before and after an environmental test, the computer program subtracted the interpolated optical-path differences of the two interferograms and produced a contour map of the difference.

Contour maps of the surface figure of two test mirrors along with the corresponding mirror interferograms are shown in figures 7 and 8. These contour maps show lines of constant surface elevation, similar to a topographical map. Neither contour map extends to the edge of the mirror, because either an adequate interpolation of the optical-path differences could not be made between a fringe and the mirror edge or the absence of optical-path-difference values beyond the mirror edge limits the interpolation scheme. These contour maps do not characterize exactly the mirror-surface figures since the effect of the nonflatness of the reference flat has not been removed from the maps. Root-mean-square and maximum peak-to-valley values for the two mirrors are also shown in figures 7 and 8. The values given in figure 7(b) are typical of those for the majority of mirror surfaces analyzed, whereas the contour maps for the mirrors differ to such a degree that no map can be considered to be typical. However, as shown in figure 7(b) for the Cer-Vit mirror, the central area of the mirror is generally elevated above the

## APPENDIX

edge for most of the mirrors analyzed. Figure 8(b) shows the contour map for a silicon mirror which is the furthest from being flat of any of the mirrors analyzed. This contour map shows a high degree of symmetry and indicates that the silicon mirror has a somewhat convex surface.

Contour maps of the figure changes determined for a beryllium-Kanigen mirror and a U.L.E. fused-silicon mirror are shown in figures 9(a) and 9(b), respectively. The contour map of figure 9(a) indicates rather small changes which are distributed randomly over the mirror area. These changes are within the error of the interferometer. In contrast to the map of figure 9(a), the map of figure 9(b) shows larger mirror changes which are distributed smoothly over the mirror area. The contour map of figure 9(b) shows a change of  $-0.015\lambda$  near the mirror edge and  $0.015\lambda$  at the center; thus, the U.L.E. fused-silica mirror has assumed a somewhat convex shape as a result of the thermal cycling.

## REFERENCES

1. Anon.: Optical Telescope Technology. NASA SP-233, 1970.
2. Anon.: Optical Materials Study Program. O.O.D. Eng. Rep. No. 41 (Contract No. DAAHO1-69-C-0950), Perkin-Elmer Corp., Feb. 1970. (Available from DDC as AD 865 842.)
3. Bradford, Alan P.; and Hass, Georg: Increasing the Far-Ultraviolet Reflectance of Silicon-Oxide-Protected Aluminum Mirrors by Ultraviolet Irradiation. J. Opt. Soc. Amer., vol. 53, no. 9, Sept. 1963, pp. 1096-1100.
4. Tolansky, S.: Multiple-Beam Interferometry of Surfaces and Films. Clarendon Press (Oxford), 1948.
5. Jones, Robert A.; and Kadakia, Pravin L.: An Automated Interferogram Analysis Technique. Appl. Opt., vol. 7, no. 8, Aug. 1968, pp. 1477-1482.
6. Goggin, W. R.; and Schroeder, J. B.: Beryllium Mirror Technology. Proceedings of the Technical Program, Electro-Optical Systems Design Conference, Karl A. Kopetzky, ed., Sept. 1969, pp. 218-224.
7. Shemanski, R. M.; Beach, J. G.; and Maringer, R. E.: Plating Stresses From Electroless Nickel Deposition on Beryllium. J. Electrochem. Soc., vol. 116, no. 3, Mar. 1969, pp. 402-409.

TABLE I.- TEST-MIRROR MATERIALS

Substrate material	Substrate manufacturer	Coatings
Fused silica (No. 7940)	Corning Glass Works	Al and MgF <sub>2</sub> Al and Si <sub>2</sub> O <sub>3</sub> <sup>a</sup>
Beryllium-Kanigen (HP-40)	Kawecki Berylco Industries, Inc.	
Cer-Vit material (premium grade C-101)	Owens-Illinois, Inc.	Al and MgF <sub>2</sub>
Silicon (polycrystalline)	Santa Barbara Research Center	Al and MgF <sub>2</sub>
U.L.E. fused silica (No. 7971)	Corning Glass Works	Al and MgF <sub>2</sub>

<sup>a</sup> O/Si  $\approx$  1.5 (ref. 3).

TABLE II.- THERMAL-CYCLING HISTORY

Type of cycle	Number of cycles	Temperature range, K	Maximum heating or cooling rate, K/min	Time for one cycle, hr
Heat	10	303 to 321	<5	8
Heat	10	303 to 321	<5	8
Heat	80	303 to 321	<5	8
Cool	10	295 to 271	<5	10
Heat	10	303 to 355	5	8
Cool	10	297 to 243	25	4
Heat	10	303 to 388	6	12
Cool	10	297 to 215	2	24
Heat	10	303 to 418	4	20
Cool	10	297 to 195	2	24

TABLE III. - RESULTS OF DIMENSIONAL-STABILITY TESTS<sup>a</sup>

(a) Aging in atmosphere

Test-mirror substrate <sup>b</sup>	Maximum fringe changes <sup>c</sup> for exposure of -											
	1 to 12 days		12 to 45 days		45 to 94 days		94 to 142 days		142 to 222 days		1 to 222 days <sup>d</sup> (total)	
	V	H	V	H	V	H	V	H	V	H	V	H
Fused silica (MgF <sub>2</sub> overcoated)	<λ/40	----	<λ/40	----	<λ/40	---	λ/40	---	λ/40	λ/40	<λ/40	<λ/40
Fused silica (Si <sub>2</sub> O <sub>3</sub> overcoated)	<λ/40	----	<λ/40	----	λ/40	---	<λ/40	---	λ/40	<λ/40	<λ/40	<λ/40
Beryllium-Kanigen	<λ/40	----	<λ/40	----	<λ/40	---	<λ/40	---	<λ/40	<λ/40	<λ/40	<λ/40
Cer-Vit	λ/40	<λ/40	λ/40	<λ/40	----	---	----	---	----	<λ/40	----	<λ/40
U.L.E. fused silica	<λ/40	----	<λ/40	----	----	---	----	---	λ/40	<λ/40	<λ/40	(λ/50) <sup>e</sup>

(b) Aging in vacuum (pressure, 10<sup>-8</sup> N/m<sup>2</sup>)

Test-mirror substrate	Maximum fringe changes after 186 days	
	V	H
Fused silica (MgF <sub>2</sub> overcoated)	<λ/40	<λ/40
Fused silica (Si <sub>2</sub> O <sub>3</sub> overcoated)	λ/40	<λ/40
Beryllium-Kanigen	λ/40	<λ/40
Cer-Vit	λ/40	λ/40
Silicon	λ/30	λ/40
(polycrystalline)		(λ/27) <sup>e</sup>
U.L.E. fused silica	<λ/40	<λ/40

<sup>a</sup> Letters V and H indicate a comparison of interferograms with vertical and horizontal fringe orientation, respectively.

<sup>b</sup> No silicon mirror was available for testing.

<sup>c</sup> Changes shown are for the intermediate aging periods noted.

<sup>d</sup> Changes shown were determined from interferograms made before and after the 222 days.

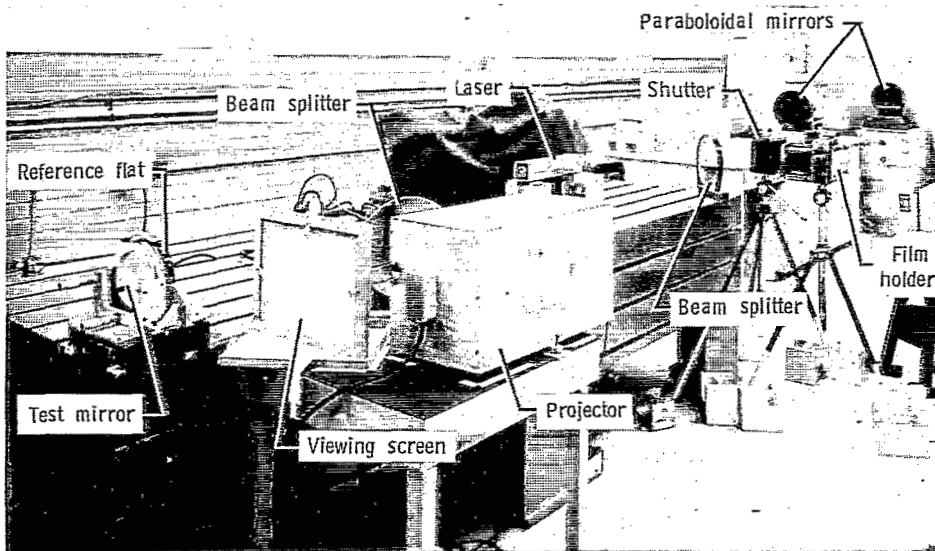
<sup>e</sup> Peak-to-valley change obtained from the automated analysis.

TABLE III.- RESULTS OF DIMENSIONAL STABILITY TESTS<sup>a</sup> - Concluded

(c) Thermal cycling

Test-mirror substrate	Maximum fringe changes <sup>b</sup> for exposure during -																			
	Cycles 11 to 20 from 303 to 321 K		Cycles 21 to 100 from 303 to 321 K		Cycles 101 to 110 from 295 to 271 K		Cycles 111 to 120 from 303 to 355 K		Cycles 121 to 130 from 297 to 243 K		Cycles 131 to 140 from 303 to 388 K		Cycles 141 to 150 from 297 to 215 K		Cycles 151 to 160 from 303 to 418 K		Cycles 161 to 170 from 297 to 195 K		Cycles 11 to 170 <sup>c</sup> (total)	
	V	H	V	H	V	H	V	H	V	H	V	H	V	H	V	H	V	H	V	H
Fused silica (MgF <sub>2</sub> overcoated)	<λ/40	<λ/40	<λ/40	<λ/40	-----	<λ/40	-----	-----	-----	-----	-----	-----	-----	-----	λ/30	λ/40	λ/40	<λ/40	λ/40	λ/40
Fused silica (Si <sub>2</sub> O <sub>3</sub> overcoated)	<λ/40	<λ/40	-----	<λ/40	-----	<λ/40	-----	<λ/40	λ/40	λ/40	<λ/40	<λ/40	<λ/40	<λ/40	<λ/40	<λ/40	λ/40	<λ/40	<λ/40	λ/40
Beryllium-Kanigen	<λ/40	<λ/40	<λ/40	<λ/40	-----	<λ/40	<λ/40	<λ/40	<λ/40	<λ/40	λ/40	<λ/40	<λ/40	<λ/40	<λ/40	<λ/40	λ/40	λ/40	<λ/40	<λ/40
Cer-Vit	<λ/40	<λ/40	λ/40	λ/40	λ/40	λ/40	λ/40	λ/40	<λ/40	<λ/40	λ/40	λ/40	λ/40	λ/40	λ/40	<λ/40	<λ/40	<λ/40	λ/40	λ/40
Silicon (polycrystalline)	<λ/40	<λ/40	-----	<λ/40	-----	<λ/40	<λ/40	<λ/40	<λ/40	<λ/40										
U.L.E. fused silica	<λ/40	<λ/40	λ/30	λ/30	<λ/40	λ/40	<λ/40	<λ/40	<λ/40	<λ/40	λ/40	λ/40	λ/40	<λ/40	λ/40	λ/40	λ/40	<λ/40	λ/40	λ/30
															(λ/43) <sup>d</sup>			(λ/38) <sup>d</sup>		(λ/29) <sup>d</sup>

<sup>a</sup> Letters V and H indicate a comparison of interferograms with vertical and horizontal fringe orientation, respectively.  
<sup>b</sup> Changes shown were determined from interferograms made before and after each set of thermal cycles.  
<sup>c</sup> Changes shown were determined from interferograms made before the 11th cycle and after the 170th cycle.  
<sup>d</sup> Peak-to-valley change obtained from the automated analysis of the interferograms.



L-70-6958.1

Figure 1.- Photograph of multiple-beam interferometer.

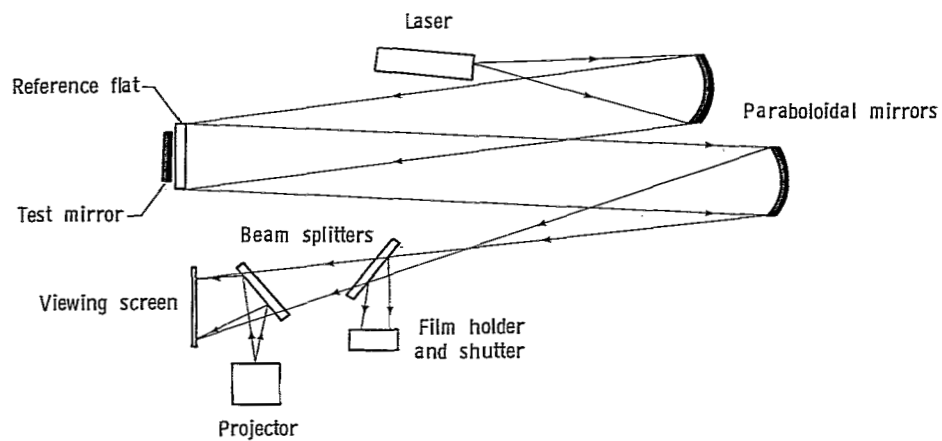
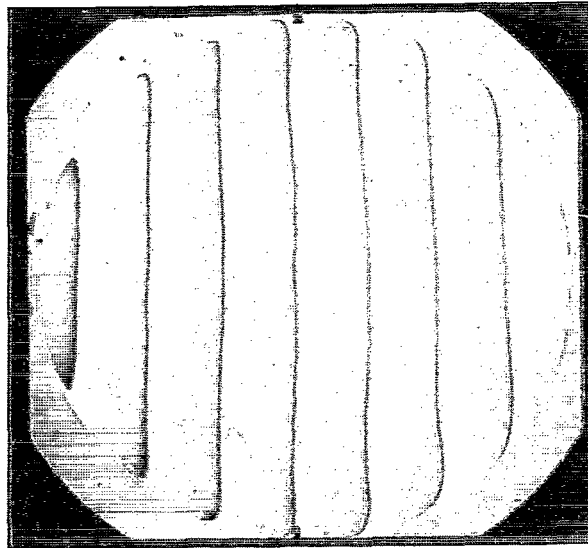
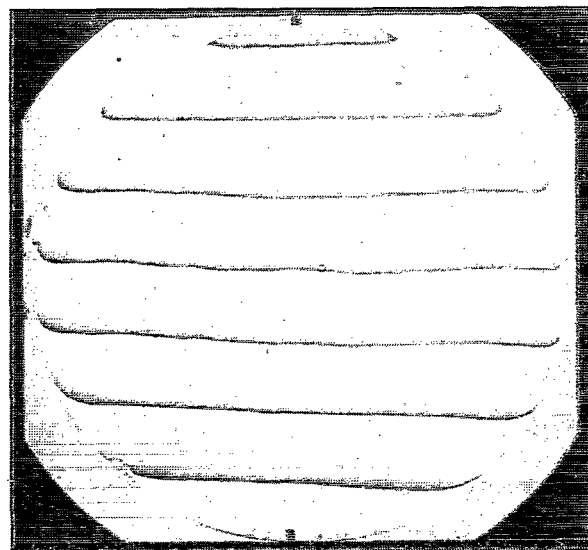


Figure 2.- Schematic of multiple-beam interferometer.



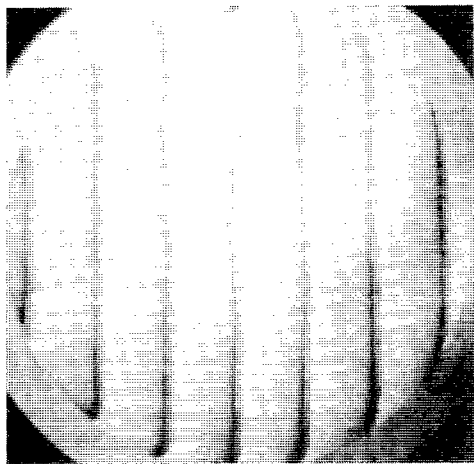
(a) Vertical.



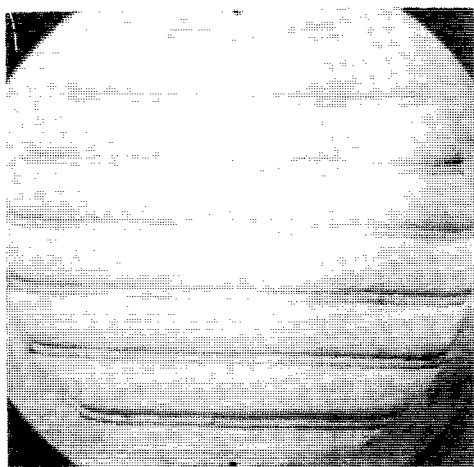
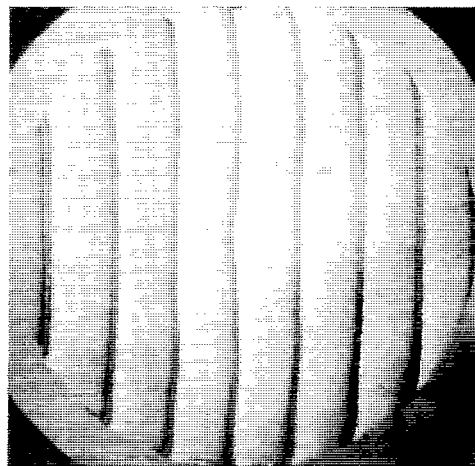
L-71-7146

(b) Horizontal

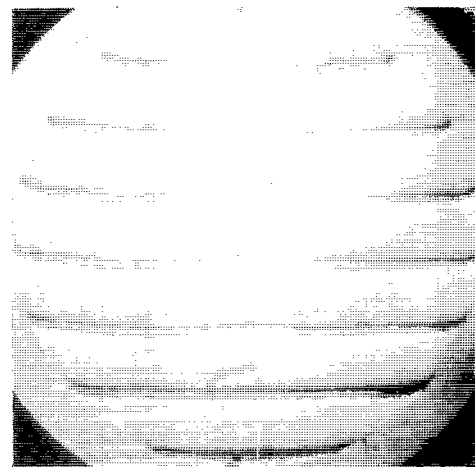
Figure 3.- Typical multiple-beam interferograms of a test mirror.



Vertical



Horizontal



L-71-7147

(a) Beryllium-Kanigen mirror.

(b) U.L.E. fused-silica mirror.

Figure 4.- Superposition of interferograms for visual analysis of mirror-configuration changes.

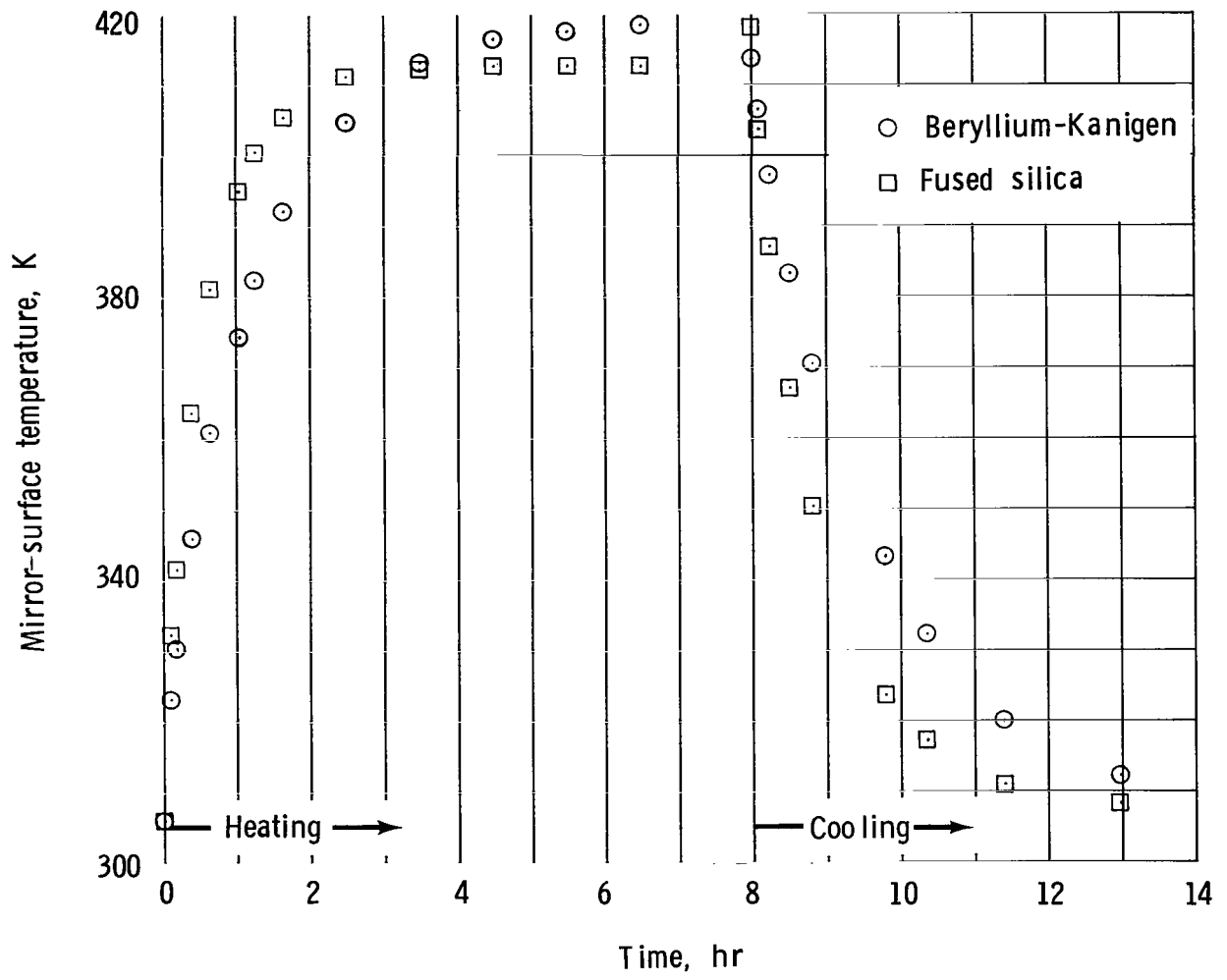
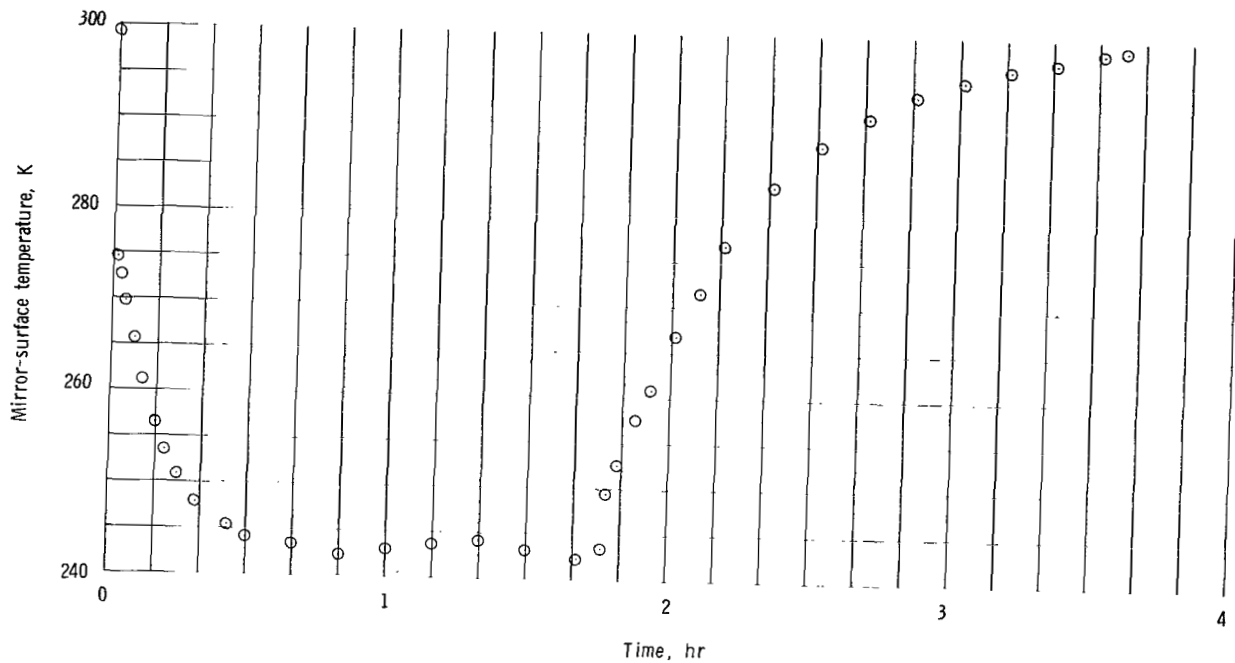
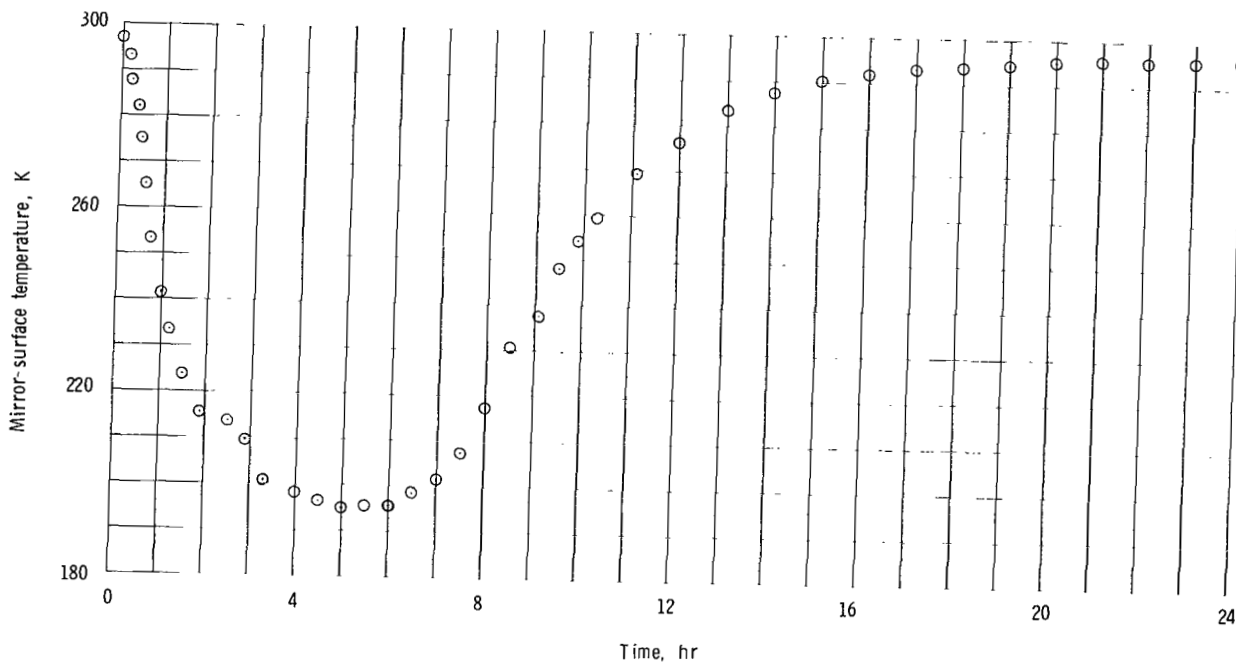


Figure 5.- Typical temperature variation for mirrors during heating and cooling phases of cycling from 306 to 418 K.

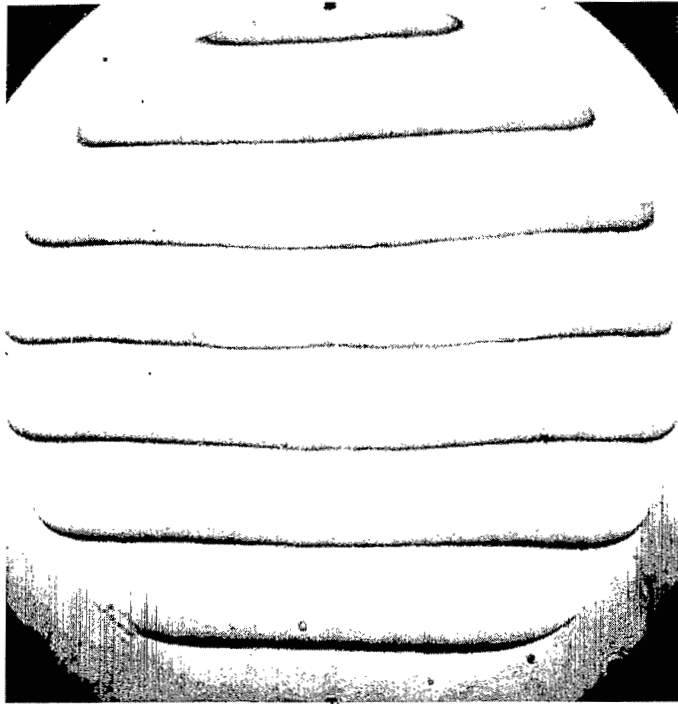


(a) Ambient temperature to 243 K.



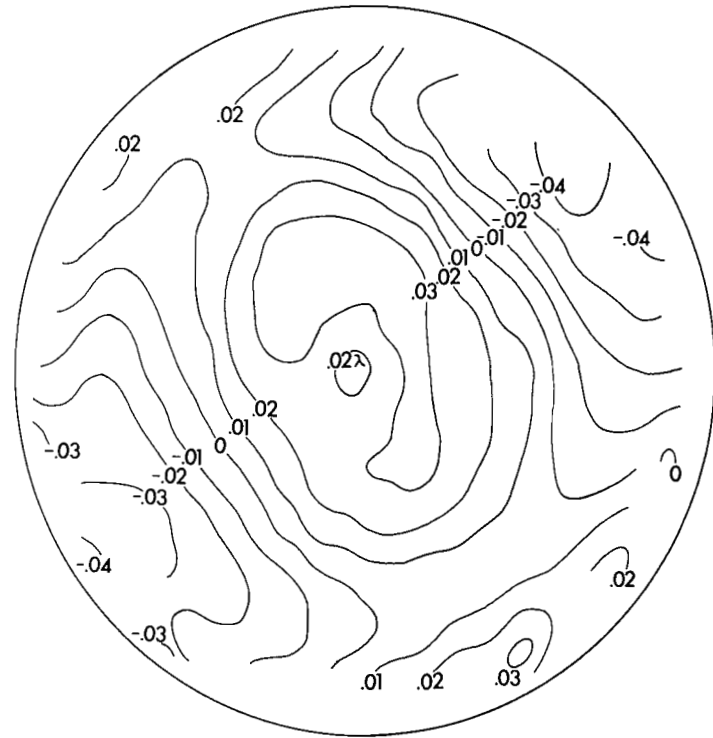
(b) Ambient temperature to 195 K.

Figure 6.- Typical temperature variation for a fused-silica mirror during cooling-cycle tests.



L-71-7148

(a) Interferogram.



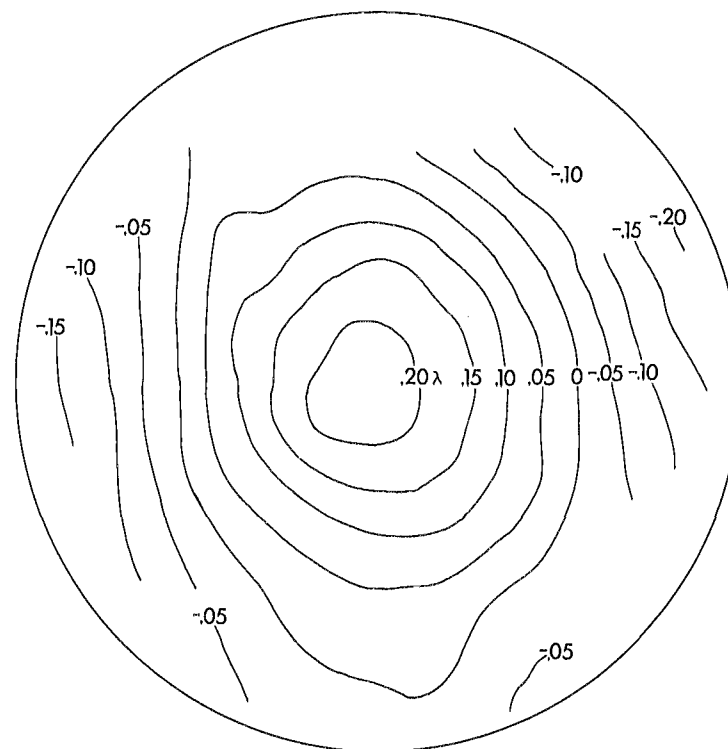
(b) Contour map (units of wavelength).

Figure 7.- Interferogram and surface contour map of Cer-Vit mirror. Peak-to-valley measurement,  $0.099\lambda$ ; root-mean-square measurement,  $0.023\lambda$ .



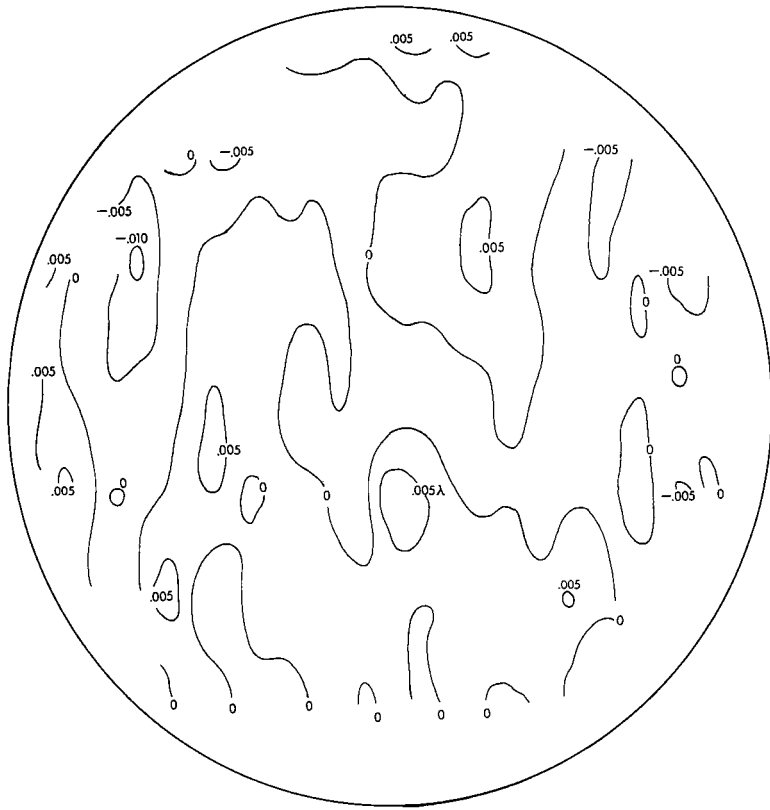
L-71-7149

(a) Interferogram.

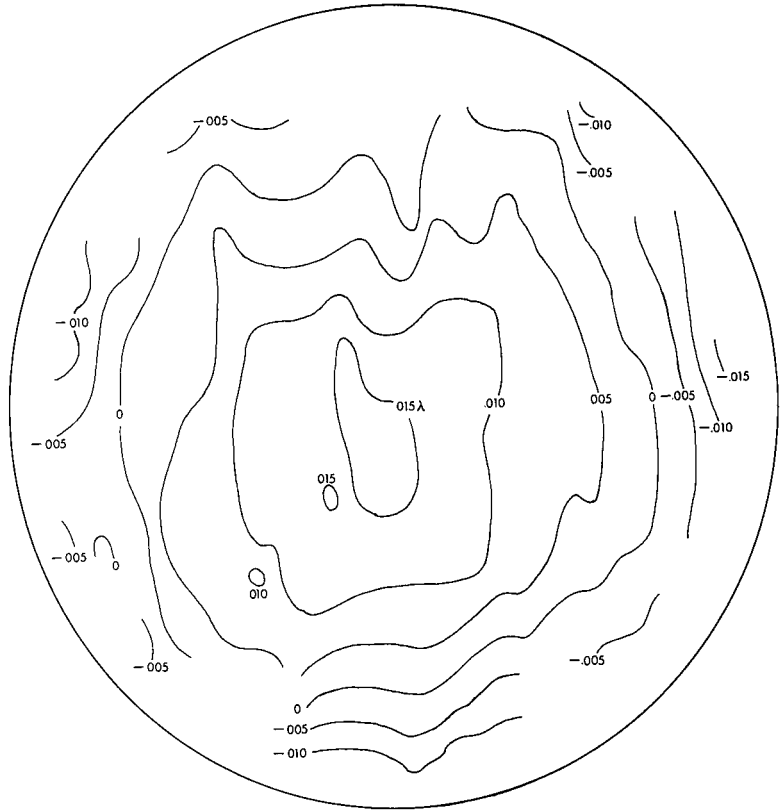


(b) Contour map (units of wavelength).

Figure 8.- Interferogram and surface contour map of silicon mirror. Peak-to-valley measurement,  $0.433\lambda$ ; root-mean-square measurement,  $0.099\lambda$ .



(a) Beryllium-Kanigen mirror.



(b) U.L.E. fused-silica mirror.

Figure 9.- Contour maps of mirror-surface changes (units of wavelength) between the 11th and 170th thermal cycles.



014 001 C1 U 18 720121 S00903DS  
DEPT OF THE AIR FORCE  
AF WEAPONS LAB (AFSC)  
TECH LIBRARY/WLOL/  
ATTN: E LOU BOWMAN, CHIEF  
KIRTLAND AFB NM 87117

POSTMASTER: If Undeliverable (Section 158  
Postal Manual) Do Not Return

*"The aeronautical and space activities of the United States shall be conducted so as to contribute . . . to the expansion of human knowledge of phenomena in the atmosphere and space. The Administration shall provide for the widest practicable and appropriate dissemination of information concerning its activities and the results thereof."*

— NATIONAL AERONAUTICS AND SPACE ACT OF 1958

## NASA SCIENTIFIC AND TECHNICAL PUBLICATIONS

**TECHNICAL REPORTS:** Scientific and technical information considered important, complete, and a lasting contribution to existing knowledge.

**TECHNICAL NOTES:** Information less broad in scope but nevertheless of importance as a contribution to existing knowledge.

**TECHNICAL MEMORANDUMS:** Information receiving limited distribution because of preliminary data, security classification, or other reasons.

**CONTRACTOR REPORTS:** Scientific and technical information generated under a NASA contract or grant and considered an important contribution to existing knowledge.

**TECHNICAL TRANSLATIONS:** Information published in a foreign language considered to merit NASA distribution in English.

**SPECIAL PUBLICATIONS:** Information derived from or of value to NASA activities. Publications include conference proceedings, monographs, data compilations, handbooks, sourcebooks, and special bibliographies.

**TECHNOLOGY UTILIZATION PUBLICATIONS:** Information on technology used by NASA that may be of particular interest in commercial and other non-aerospace applications. Publications include Tech Briefs, Technology Utilization Reports and Technology Surveys.

*Details on the availability of these publications may be obtained from:*

**SCIENTIFIC AND TECHNICAL INFORMATION OFFICE**

**NATIONAL AERONAUTICS AND SPACE ADMINISTRATION**

**Washington, D.C. 20546**